Activation of RhoA-ROCK-BMP signaling reprograms adult human corneal endothelial cells

Ying-Ting Zhu,[1] Fu Li,[2] Bo Han,[3] Sean Tighe,[1] Suzhen Zhang,[1] Szu-Yu Chen,[1] Xin Liu,[3] and Scheffer C.G. Tseng[1]

[1]TissueTech, Inc., Ocular Surface Center, and Ocular Surface Research & Education Foundation, Miami, FL 33173
[2]Pediatric Research Institute and Department of Pediatric Hematology, Qilu Children's Hospital, Shandong University, Jinan, Shandong 250022, People's Republic of China
[3]Department of Ophthalmology, Union Hospital, Tongji Medical College, Huazhong University of Science and Technology, Wuhan, Hubei 430022, People's Republic of China

Currently there are limited treatment options for corneal blindness caused by dysfunctional corneal endothelial cells. The primary treatment involves transplantation of healthy donor human corneal endothelial cells, but a global shortage of donor corneas necessitates other options. Conventional tissue approaches for corneal endothelial cells are based on EDTA-trypsin treatment and run the risk of irreversible endothelial mesenchymal transition by activating canonical Wingless-related integration site (Wnt) and TGF-β signaling. Herein, we demonstrate an alternative strategy that avoids disruption of cell–cell junctions and instead activates Ras homologue gene family A (RhoA)–Rho-associated protein kinase (ROCK)–canonical bone morphogenic protein signaling to reprogram adult human corneal endothelial cells to neural crest–like progenitors via activation of the miR302b-Oct4-Sox2-Nanog network. This approach allowed us to engineer eight human corneal endothelial monolayers of transplantable size, with a normal density and phenotype from one corneoscleral rim. Given that a similar signal network also exists in the retinal pigment epithelium, this partial reprogramming approach may have widespread relevance and potential for treating degenerative diseases.

Introduction

Human corneal endothelial cells (HCECs) embryonically derived from cranial neural crest cells form a single monolayer of hexagonal cells on the Descemet's membrane of the posterior cornea. By exerting effective barrier and pump functions, HCECs play a pivotal role in regulating corneal stromal hydration and hence transparency (for reviews see Bonanno, 2003; Fischbarg and Maurice, 2004). Unlike other species, HCECs are notorious for having limited proliferative capacity in vivo (Laing et al., 1984) because of the mitotic block at the G1 phase of the cell cycle due to "contact inhibition" (Joyce, 2005). Consequently, diseases, aging, injuries, or surgeries frequently result in corneal blindness as a result of HCEC dysfunction, which presents with either insufficient numbers/density in "bullous keratopathy" (for review see Bourne and McLaren, 2004) or endothelial-mesenchymal transition (EMT) in "retrocorneal fibrous membrane" (Lee and Kay, 2006).

To circumvent the mitotic block governed by contact inhibition, the conventional engineering method is to disrupt cell–cell junctions with EDTA-trypsin to generate single HCECs and then culture them in a medium supplemented with growth factors including basic FGF (bFGF; Engelmann et al., 1988; Chen et al., 2001; Ishino et al., 2004; Mimura et al., 2004; Yokoo et al., 2005; Hsiue et al., 2006; Sumide et al., 2006; Li et al., 2007; Hatou et al., 2013). Unfortunately, this method runs the risk of losing the normal phenotype to EMT (Lee and Kay, 2006; Zhu et al., 2012). We have reported that one mechanism leading to EMT is caused by the activation of canonical Wingless-related integration site (Wnt) and TGF-β signaling (Zhu et al., 2012).

To mitigate this shortcoming, we have discovered a novel strategy to unlock the mitotic block in HCEC monolayers, without disrupting cell–cell junctions, by knockdown of p120 catenin (p120) to activate p120–Ras homologue gene family A

Correspondence to Scheffer C.G. Tseng: stseng@ocularsurface.com

Abbreviations used in this paper: bFGF, basic FGF; BMP, bone morphogenic protein; BMPR, BMP receptor; EMT, endothelial-mesenchymal transition; ESC, embryonic stem cell; HCEC, human corneal endothelial cell; ID, inhibitor of differentiation; iPSC, induced pluripotent stem cell; LIF, Leukemia inhibitory factor; LEF1, lymphoid enhancer–binding factor 1; MESCM, modified ESC medium; p120, p120 catenin; Rho, Ras homologue gene family; ROCK, Rho-associated protein kinase; scRNA, scrambled RNA; SHEM, supplemental hormonal epithelial medium; Wnt, Wingless-related integration site; ZO-1, Zona occludens protein 1.

Supplemental material can be found at:
http://doi.org/10.1083/jcb.201404032

The Rockefeller University Press $30.00
J. Cell Biol. Vol. 206 No. 6 799–811
www.jcb.org/cgi/doi/10.1083/jcb.201404032

(RhoA)–Rho-associated protein kinase (ROCK) signaling while sparing canonical Wnt signaling (Zhu et al., 2012). We have used this strategy to successfully engineer HCEC monolayers to a mean size of 2.1 ± 0.4 mm in diameter from Descemet's membrane stripped from 1/8 of the corneoscleral rim normally discarded after conventional corneal transplantation (Zhu et al., 2012). Subsequently, we further optimized the knockdown regimen of p120 siRNA regarding dosing, frequency, and starting time, and noted that knockdown with siRNAs to both p120 and Kaiso, which is a transcriptional repressor released by nuclear translocation of p120, starting from day 7, further expanded the HCEC monolayer size to 5.0 ± 0.3 mm in diameter after 5 wk of culture in supplemental hormonal epithelial medium (SHEM; see Materials and methods for the medium composition; Zhu et al., 2014). This success is accompanied by the activation of RhoA-ROCK-noncanonical bone morphogenic protein (BMP) signaling (Zhu et al., 2014).

To further investigate how to expand the HCEC monolayers to a transplantable size, i.e., at least 8 mm in diameter, we switched SHEM to a serum-free medium termed modified embryonic stem cell medium (MESCM; see Materials and methods for the medium composition), which is used in our laboratory to expand limbal stromal niche progenitor cells (Xie et al., 2011, 2012; Li et al., 2012a,b). Herein, we report our success in using this optimized knockdown with p120-Kaiso siRNAs to expand HCEC monolayers in MESCM to the mean size of 11.0 ± 0.6 mm from Descemet's membrane stripped from one eighth of the corneoscleral rim. This success is achieved by reprogramming adult HCECs into neural crest–like progenitors via activation RhoA-ROCK-canonical BMP signaling that links to the activation of the miR302b-Oct4-Sox2-Nanog network.

Results

Disruption of intercellular junctions leads to the loss of the normal HCEC phenotype by activation of canonical Wnt signaling

In the in vitro model system of contact-inhibited HCEC monolayers (Li et al., 2007; Zhu et al., 2008), a brief exposure to 5 mM EDTA for 1 h alone leads to notable disruption of the intercellular junction (Zhu et al., 2012). If 20 ng/ml bFGF is immediately added for 2 d, 10 ng/ml TGF-β1 is added for 3 d, or 20 ng/ml bFGF is added for 2 d followed by 10 ng/ml TGF-β1 for 3 d, HCECs transform into fibroblastic-like cells due to EMT (Zhu et al., 2012). This pathological consequence is causatively linked to the activation of RhoA-ROCK signaling that is coupled with canonical Wnt signaling (under bFGF and/or EGF) and canonical TGF-β-pSmad2/3/Zeb1/2 signaling (under TGF-β1; Zhu et al., 2012). Herein, we further showed that treatment of trypsin/EDTA for as brief as 5 min induced a "fibroblastic" appearance in contact-inhibited HCEC monolayers within 24 h and that cells failed to fully recover the hexagonal shape even after 28 d in EGF-containing SHEM (Fig. 1 A). This morphological alteration was accompanied by activation of canonical Wnt signaling, as indicated by nuclear localization of β-catenin and lymphoid enhancer–binding factor 1 (LEF1; Fig. 1 A), four- and sixfold increase of mRNA expression of β-catenin and LEF1 (Fig. 1 B), 13- and 15-fold increase of nuclear protein of β-catenin and LEF1 (Fig. 1 C), and 17-fold increase of the TCF/LEF promoter activity (Fig. 1 D). In contrast, HCEC monolayers treated by p120 siRNA or p120-Kaiso siRNAs retained a hexagonal shape without nuclear staining of β-catenin and LEF1, without increased mRNA expression of β-catenin and LEF1, and without the increased promoter activity of TCF/LEF1 (Fig. 1), which supports the lack of activation of canonical Wnt signaling.

Knockdown with p120-Kaiso siRNAs in MESCM leads to activation of RhoA-ROCK-canonical BMP signaling

Recently, we reported that knockdown by p120-Kaiso siRNAs in SHEM helped expand HCEC monolayers by activation of RhoA-ROCK-noncanonical BMP signaling that leads to nuclear translocation of pNF-kB (p65, S276; Zhu et al., 2014). Because MESCM has been routinely used in our laboratory to expand limbal stromal niche progenitor cells (Xie et al., 2011, 2012; Li et al., 2012a,b), we switched SHEM to MESCM and screened whether RhoA-ROCK-BMP signaling was also involved by adding CT-04 to inhibit RhoA, ROCK1/2 siRNAs (more specific to target ROCK1 and ROCK2 than Y27632) to down-regulate both ROCK1 and ROCK2, and Noggin to inhibit BMP signaling. All three inhibitors completely inhibited BrdU labeling induced by p120-Kaiso knockdown in HCEC monolayers (Fig. 2 A). Further analysis confirmed that the RhoA-GTP level was indeed activated by p120 siRNA and further by p120-Kaiso siRNAs in MESCM (Fig. 2 B), similar to SHEM (Zhu et al., 2012, 2014). In addition, both p120 siRNA and p120-Kaiso siRNAs up-regulated BMP3, BMP4, and BMP6 (but not BMP2, BMP7, and BMP9) as well as BMP receptor 1A (BMPR1A) and BMPR2 (but not BMPR1B) transcripts (Fig. 2 C). Activation of canonical BMP signaling was confirmed by marked up-regulation of inhibitor of differentiation 1 (ID1) and (to a lesser extent) ID2-4 (Hollnagel et al., 1999; Fig. 2 D), and nuclear translocation of pSMAD1/5/8 (Fig. 2 E). These responses were blocked by CT-04, ROCK1/2 siRNAs, or Noggin (Fig. 2 E). Additionally, nuclear translocation of pNF-kB (p65, S276) that was noted after activation of noncanonical BMP signaling (Zhu et al., 2014) when cultured in SHEM (Fig. 2 F, red) was not observed when cultured in MESCM (Fig. 2 F, green).

BMP signaling leads to marked expansion via reprogramming of HCECs to neural crest–like progenitors

Without p120-Kaiso knockdown, the size of HCEC monolayers in diameter was promoted from 1.4 ± 0.1 mm in SHEM to 4.4 ± 0.3 mm in MESCM in 6 wk (Fig. 3 A, $n = 4$). With p120-Kaiso knockdown, MESCM dramatically expanded the size of HCEC monolayers in diameter from 5.0 ± 0.3 mm in SHEM to 11.0 ± 0.6 mm, i.e., a transplantable size (Fig. 3 B, $P < 0.05$, $n = 4$). BrdU-labeled nuclei were found in the mid-periphery and the periphery of HCEC monolayers by week 6 only in MESCM (Fig. 3 C, $n = 4$). These results have been replicated four times from a total of 24 donors. Unlike the effects seen in SHEM (Fig. S3), MESCM's growth-promoting effect was coupled with

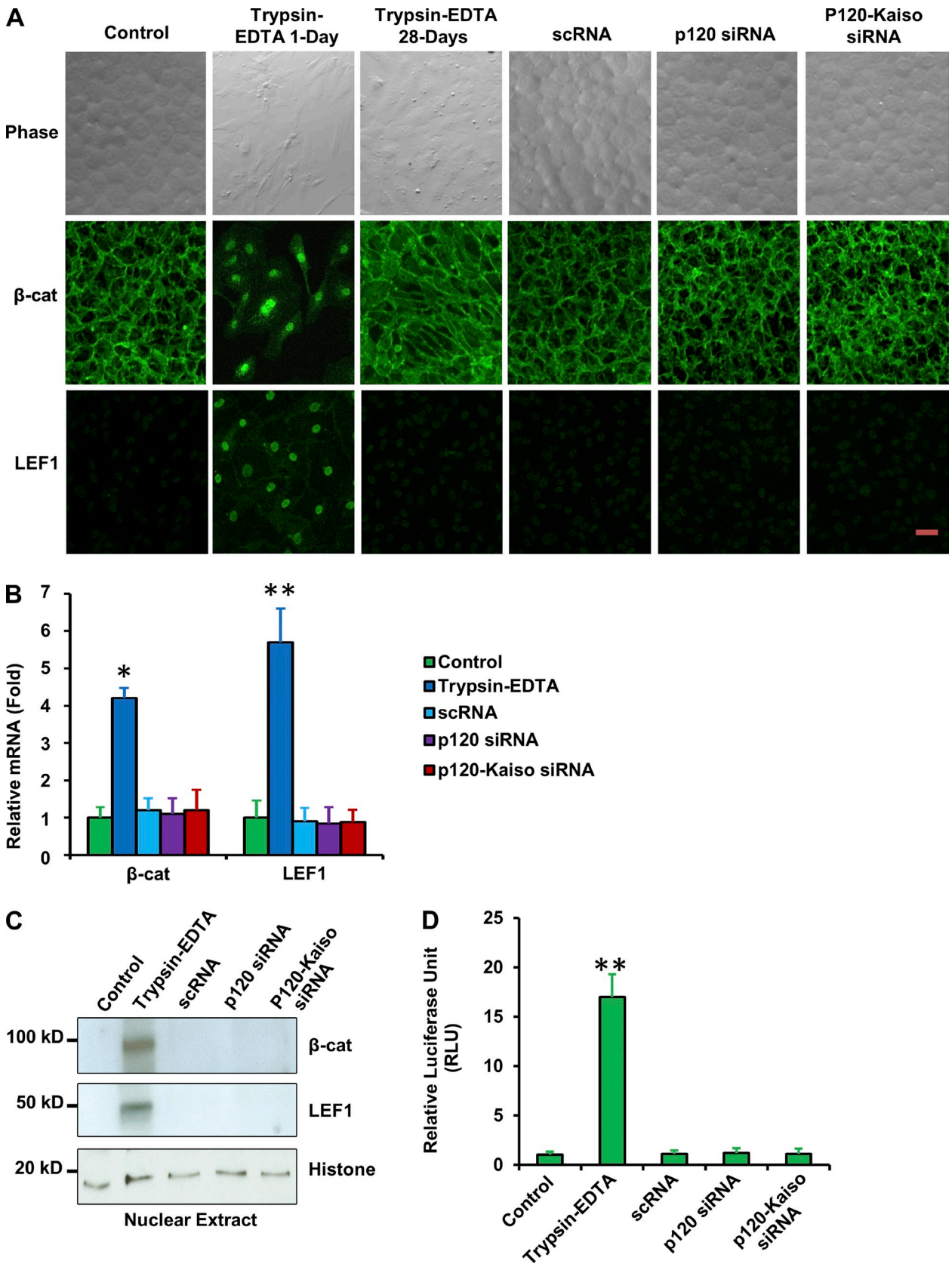

Figure 1. **Activation of canonical Wnt signaling by trypsin/EDTA but not by p120-Kaiso knockdown.** Contact-inhibited HCEC monolayers cultured at 14 d in SHEM were treated with trypsin/EDTA for 5 min, or knockdown with p120 siRNA or p120-Kaiso siRNAs weekly for 4 wk. The resultant cells were investigated by phase-contrast microscopy, immunofluorescence staining of β-catenin and LEF1 (both green; A), qRT-PCR of β-catenin and LEF1 transcripts (48 h later; B), Western blotting of nuclear extracts (48 h later, using histone as the loading control; C), and TCF/LEF promoter activity (24 h later; D). *, $P < 0.05$; **, $P < 0.01$. $n = 4$. Error bars indicate ±SEM. Bar, 25 μm.

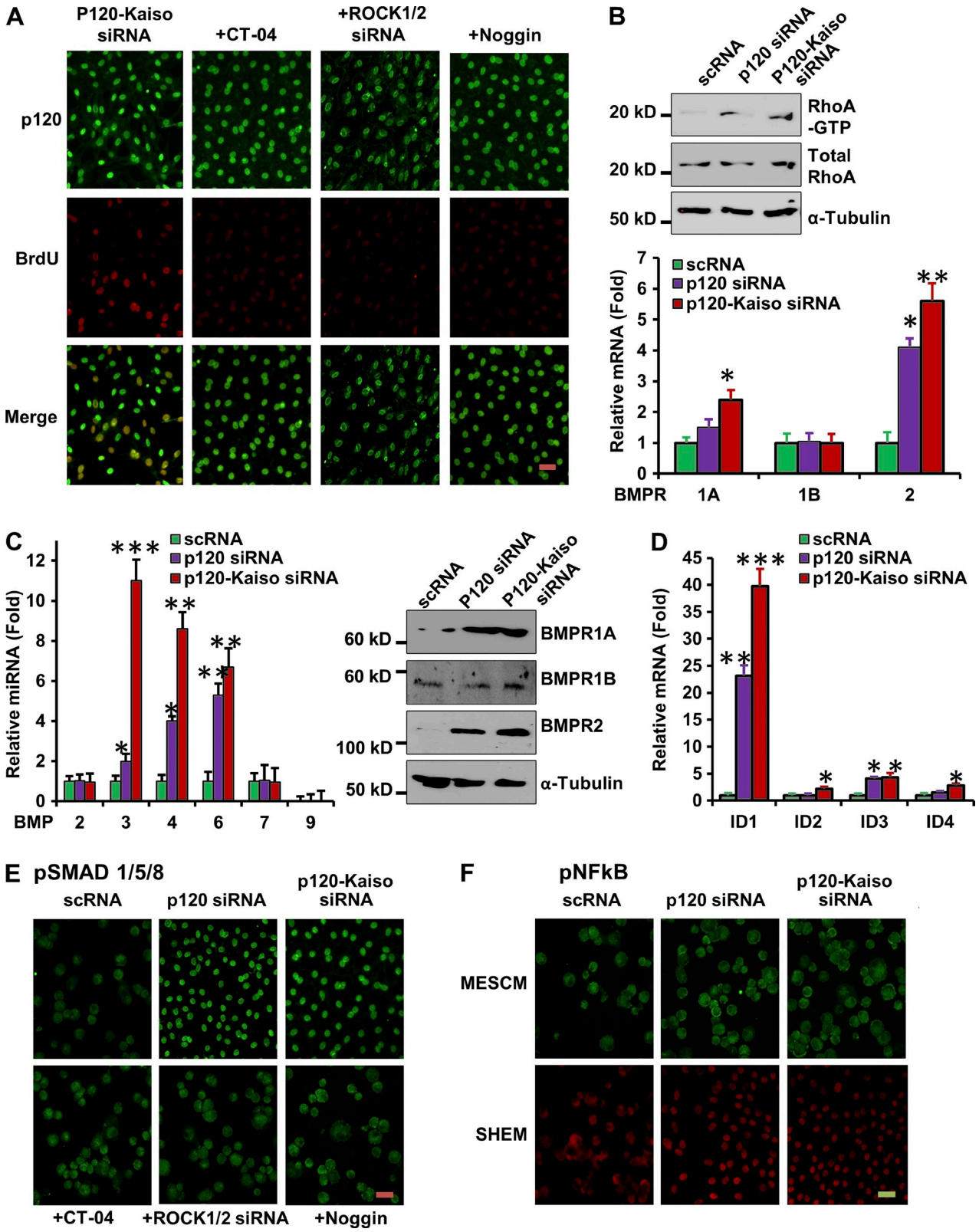

Figure 2. **p120-Kaiso knockdown in MESCM activates RhoA-ROCK-canonical BMP signaling to unlock the mitotic block.** (A) HCEC monolayers obtained by weekly knockdown with p120-Kaiso siRNAs after 1 wk of culturing for 5 wk. BrdU-labeled nuclei (red) with double labeling with p120 (green) were abolished by CT-04, ROCK1/ROCK2 siRNAs, or Noggin. (B) RhoA-GTP was increased by p120 siRNA and further increased by p120-Kaiso siRNAs (*, $P < 0.05$; **, $P < 0.01$). $n = 4$, compared with scRNA and normalized by α-tubulin. (C and D) Expression of BMP ligands, receptors (C), and BMP downstream genes, ID1-4 (D), was measured by qRT-PCR and Western blotting (*, $P < 0.05$; **, $P < 0.01$; $n = 4$, compared with scRNA). Error bars indicate ±SEM. (E and F) Immunofluorescence staining of pSMAD1/5/8 (green) and pNF-κB (green in MESCM, red in SHEM) was performed to examine the canonical BMP signaling (E) and noncanonical BMP signaling (F), respectively. In E, CT-04, ROCK1/2 siRNA, or Noggin were added to p120-Kaiso siRNA. Bars, 25 μm.

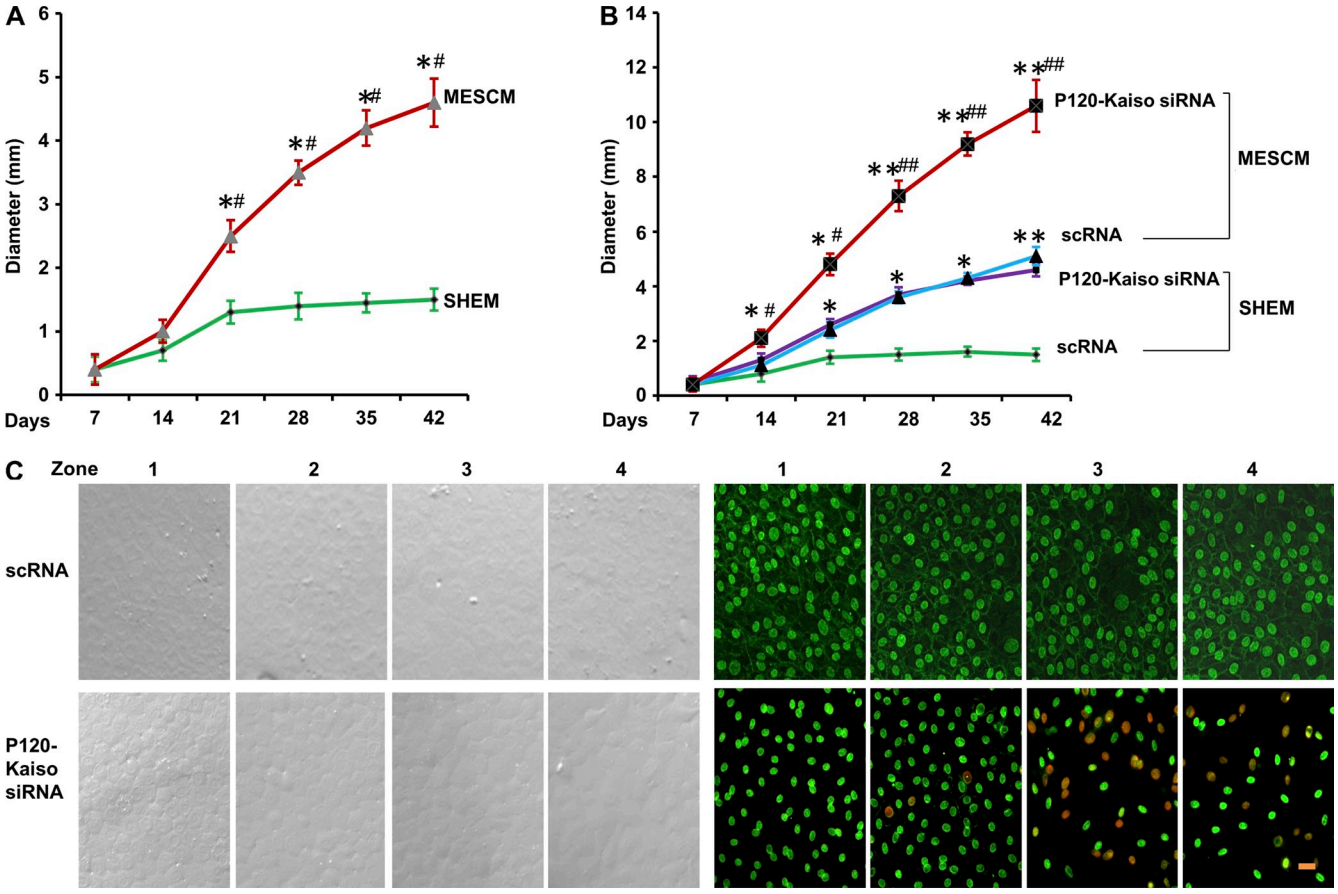

Figure 3. **Successful expansion of HCEC monolayers by knockdown with p120-Kaiso siRNAs in MESCM.** (A and B) The size of HCEC monolayers in diameter was measured when cultured in SHEM and MESCM without (A; *, $P < 0.05$, $n = 4$, when compared with SHEM) or with knockdown by 100 nM of scRNA or p120-Kaiso siRNAs (B; *, $P < 0.05$; **, $P < 0.01$ when compared with their corresponding scRNA controls; #, $P < 0.05$; ##, $P < 0.01$ when compared with SHEM, $n = 4$). Error bars indicate ±SEM. (C) BrdU-labeled nuclei (red) were only detected in those treated with p120-Kaiso siRNAs in MESCM ($P < 0.01$, compared with their corresponding scRNA control in MESCM in zone 3 and zone 4, which were 50% and 40%, respectively, when equally subdivided into four zones from the center after 6 wk of culturing, i.e., 5 wk after weekly knockdown). Bar, 25 µm.

higher transcript expression of embryonic stem cell (ESC) markers such as Oct4, Sox2, Nanog, Nestin, and SSEA4 (Fig. 4 A) and that of neural crest markers, such as AP2β, FOXD3, and SOX9 (Fig. 4 B). Expression of these markers was completely blocked by Noggin, which indicates that the reprogramming is controlled by BMP signaling. Correspondingly, positive nuclear immunostaining staining of Nanog, Oct 4, and SOX2 as well as positive membranous and cytoplasmic staining of Nestin, SSEA4, SOX9, and FOXD3 were observed in HCECs receiving the knockdown of p120 siRNA or p120-Kaiso siRNAs (Fig. 4 D). A transcription complex made of Oct4-Nanog-Sox2 has been identified to trigger expression of the miR302 cluster as a positive regulatory network essential for reprogramming of induced pluripotent stem cells (iPSCs; Anokye-Danso et al., 2011; Lin et al., 2011; Miyoshi et al., 2011). Because expression of miR302b and miR302c was down-regulated by ROCK1 siRNA and ROCK2 siRNA in a mouse endothelial cell model (Stiles et al., 2013), we investigated their expression and found that expression of miR302b and miR302c was increased five- or eightfold, and two- or twofold in HCECs after knockdown by p120 siRNA or p120-Kaiso siRNAs, respectively (Fig. 4 C). Furthermore, overexpression of miR302b and miR302c, nuclear translocation of ESC markers, and positive expression of neural crest markers were all blocked by Noggin (Fig. 4). Collectively, these findings support the notion that BMP signaling is responsible for the reprogramming of HCECs to neural crest–like progenitor cells. Because Noggin also blocked BrdU labeling (Fig. 2), we suggest that effective expansion of HCEC monolayers is achieved by activating canonical BMP signaling in MESCM, but not in SHEM, through the reprogramming of HCEC progenitors.

Reprogramming and expression of miRNA302 are controlled by RhoA-ROCK-BMP signaling

To confirm whether the reprogramming promoted by p120-Kaiso siRNAs was indeed through activation of RhoA-ROCK-canonical BMP signaling, we added Rho inhibitor, CT-04, ROCK1/2 siRNAs, or the BMP inhibitor Noggin. The results showed that they all abolished up-regulation of BMP3, BMP4, and BMP6; overexpression of BMPR1A and BMPR2; and up-regulation of ID1-4 transcripts by p120-Kaiso siRNAs (Fig. 5 A). Expression of BMPR1B, which was not up-regulated by p120-Kaiso siRNAs, was actually up-regulated by ROCK1 and ROCK2 siRNAs. Overexpression of miR302b was also abolished by

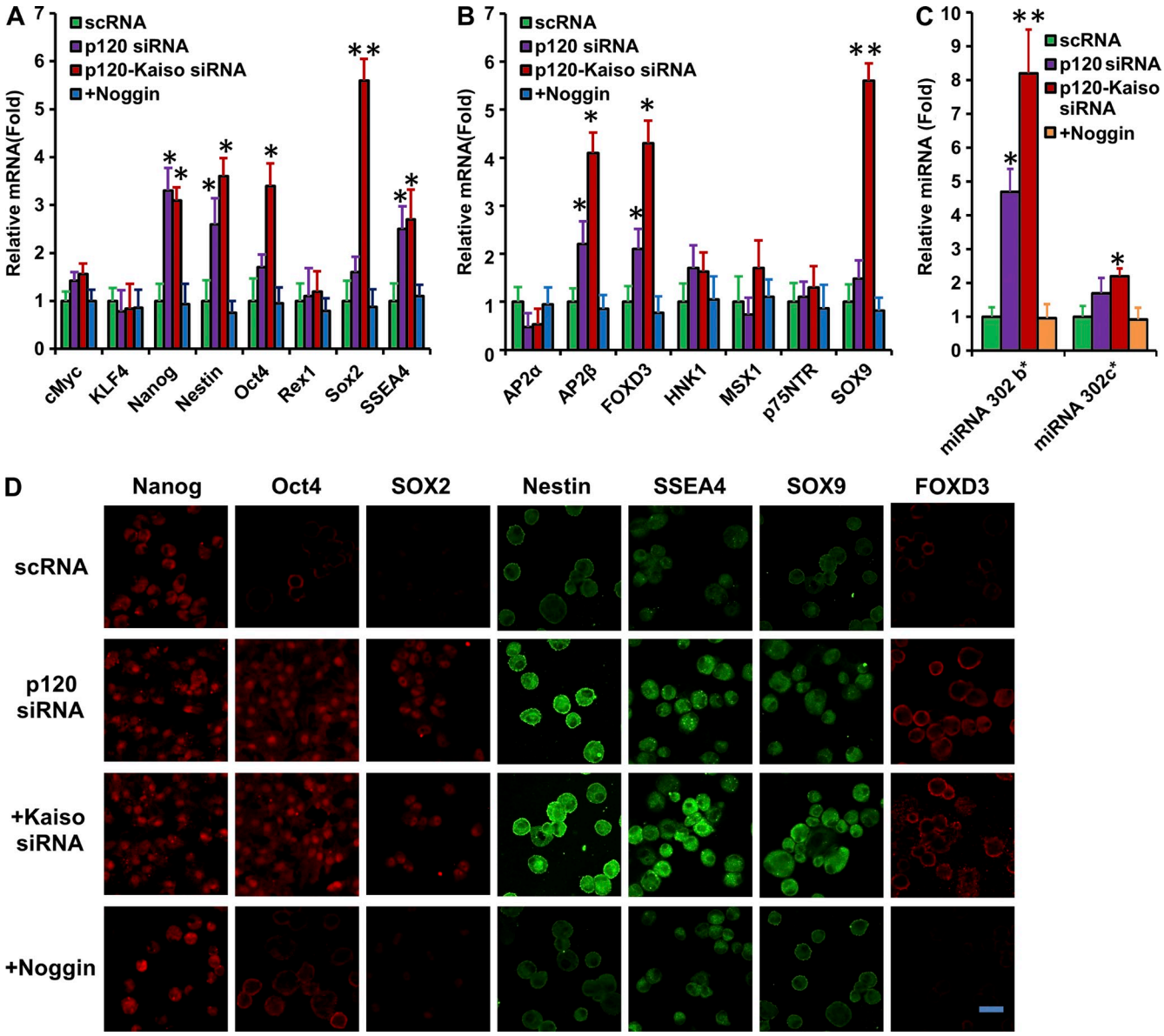

Figure 4. **Expression of markers of neural crest and ESCs and miR302 by knockdown with p120 or p120-Kaiso siRNAs in MESCM.** HCEC monolayers were cultured in MESCM under weekly knockdown by p120 siRNA or p120-Kaiso siRNAs starting from 1 wk of culturing. (A–C) Transcript expression of ESC markers (A), neural crest cell markers (B), and miR302 (C) was measured by qRT-PCR after 5 wk of culturing (*, $P < 0.05$, **, $P < 0.01$, $n = 4$, when compared with the corresponding scRNA control). Such overexpression was abolished by Noggin added in the final week of culturing (A and B). Error bars indicate ±SEM. (D) Immunostaining of nuclear expression of Nanog, Oct4, and Sox 2 as well as membranous and cytoplasmic expression of Nestin, SSEA4, SOX9, and FOXD3 was also compared. Bar, 25 µm.

CT-04, ROCK1 and ROCK2 siRNA, or Noggin, whereas overexpression of miR302c was suppressed by CT-04 and Noggin but not ROCK1 or ROCK2 siRNA (Fig. 5 B). Overexpression of Nanog, Nestin, and SSEA4 was also abolished by these three inhibitors, whereas that of Oct4 was suppressed by CT-04, ROCK1 siRNA, and Noggin but not ROCK2 siRNA, and that of Sox2 was actually suppressed by Noggin and further by ROCK2 siRNA (below the level of scrambled RNA [scRNA]) but not CT-04 and ROCK1 siRNA (Fig. 5 C). Overexpression of AP2β and SOX9 was similarly suppressed by three inhibitors, whereas that of FOXD3 was suppressed by CT-04, ROCK1 siRNA, and Noggin but not ROCK2 siRNA (Fig. 5 D). These results collectively support the notions that activation of canonical BMP signaling by p120-Kaiso knockdown in MESCM is responsible for the aforementioned reprogramming and up-regulation of miR302b and miR302c. Although RhoA-ROCK signaling was also required for nuclear translocation of pSMAD1/5/8 and nuclear BrdU labeling (Fig. 2), our further analysis showed that both ROCK1 and ROCK2 acted differently from Noggin and CT-04 in regulating BMP signaling; e.g., expression of BMPR1B, miR302c, and ROCK1 differed from ROCK2 in regulating Oct4, Sox2, and FOXD3.

Withdrawal of p120-Kaiso knockdown maintains the normal HCEC phenotype

We have reported that withdrawal of knockdown by p120 siRNA in SHEM retains the in vivo HCEC morphology, density, and

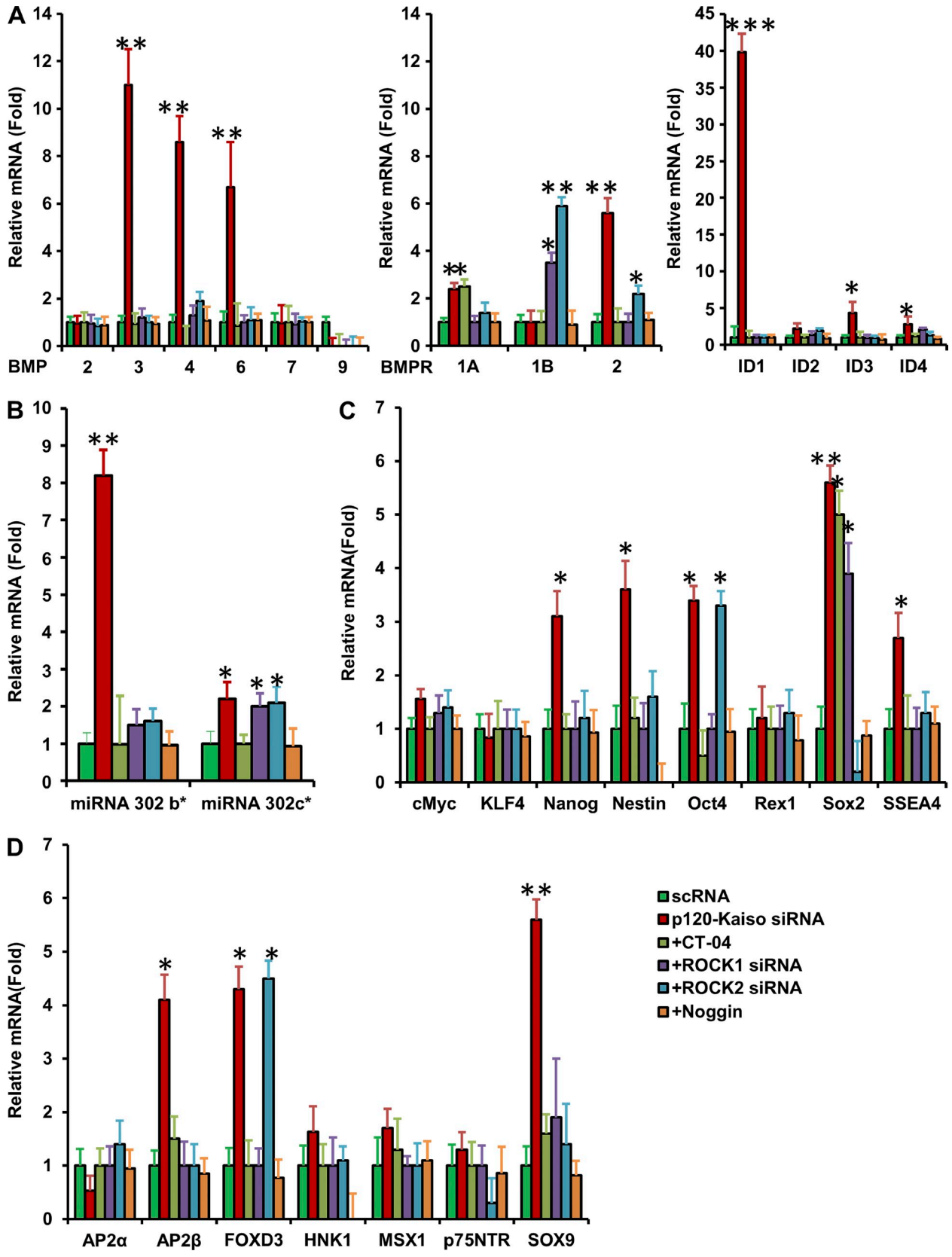

Figure 5. **Reprogramming and expression of miR302b are attenuated by the Rho inhibitor CT-04, ROCK1/2 siRNAs, or Noggin.** HCEC monolayers were cultured in MESCM under weekly knockdown by p120 siRNA or p120-Kaiso siRNAs starting from 1 wk, and various inhibitors were added for the last week of culturing. Transcript expression of BMPs, BMPRs, IDs (A), miR302b and miR302c (B), ESC markers (C), and neural crest cell markers (D) was measured by qRT-PCR after 5 wk of culturing (*, $P < 0.05$; **, $P < 0.01$; ***, $P < 0.001$; $n = 4$, when compared with the p120-Kaiso siRNAs by setting the expression level of scRNA as 1). Error bars indicate ±SEM.

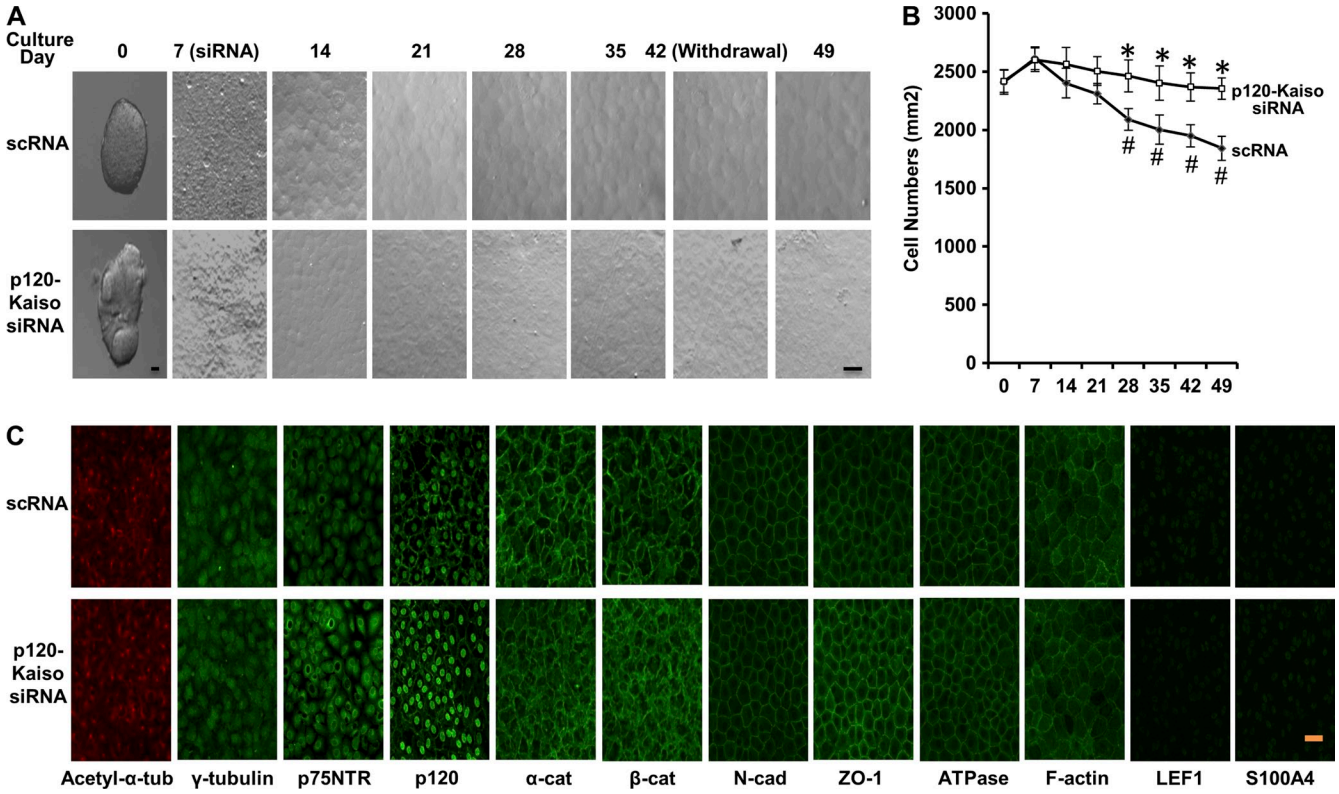

Figure 6. **Maintenance of normal HCEC shape, density, and phenotype after withdrawal of p120-Kaiso siRNAs.** (A and B) The morphology (A) and the density (B; *, $P < 0.05$ compared with the scRNA control; #, $P < 0.05$ compared with the in vivo density; $n = 4$) of HCEC monolayers were monitored throughout the entire period. Error bars indicate ±SEM. (C) Immunofluorescence staining to acetyl-α-tubulin (red) and other markers (all green) was performed in HCEC monolayers 1 wk after withdrawal. Bars, 25 µm.

phenotype (Zhu et al., 2012, 2014). Hence, we would like to verify that such withdrawal also achieved the same result for the knockdown by p120-Kaiso siRNAs in MESCM. Compared with the in vivo stripped Descemet's membrane, the resultant cell shape remained hexagonal during the entire knockdown period (5 wk of weekly treatment after the first week of culture followed by withdrawal for 1 wk) for HCEC monolayers treated with scRNA or p120-Kaiso siRNAs (Fig. 6 A). The resultant cell density was also maintained at the in vivo level by p120-Kaiso siRNAs in MESCM, but was decreased, however, by scRNA after 6 wk of culturing (Fig. 6 B). 1 wk after withdrawal, the resultant HCEC monolayer retained the centric expression of acetylate-α-catenin (a marker of the basal body and the primary cilium; Blitzer et al., 2011), uniform cytoplasmic expression of γ-tubulin and p75NTR (of which the latter is considered a marker of neural crest cells; Wong et al., 2006), and junctional expression of p120, N-cadherin, α-catenin, β-catenin, Zona occludens protein 1 (ZO-1), Na-K-ATPase, and F-actin (all are markers of HCECs), without expression of LEF1 and S100A4 (both are markers of EMT; Zhu et al., 2012; Fig. 6 C). Such expression of HCEC markers was consistent with the in vivo expression pattern previously reported by us (Zhu et al., 2012, 2014).

Because enhanced nuclear p120 levels are noted in several tumor cell lines (Daniel, 2007), we examined the change in RhoA-ROCK-canonical BMP signaling and the expression of markers for neural crest–like progenitors 1 wk after withdrawal of p120-Kaiso siRNAs. Our results showed that withdrawal of p120-Kaiso siRNAs resulted in cessation of RhoA activation (Fig. S1 A), BMP signaling (significant reduction of BMPR1A and abolition of BMPR2; Fig. S1 B), nuclear translocation of p120, and labeling of BrdU (Fig. S1 E). Furthermore, transcript expression of the markers for both ESCs (Fig. S1 C) and neural crest cells (Fig. S1 D) was also aborted. These findings confirmed that HCEC progenitors reverted to an in vivo phenotype, whereas RhoA activation and BMP signaling become inactive.

Discussion

Perturbation of contact inhibition to unlock the mitotic block of HCECs can be achieved by the use of EDTA/trypsin to disrupt intercellular (adherent) junctions (Senoo et al., 2000; Patel and Bourne, 2009). In the presence of bFGF (Kay et al., 1998; Lee et al., 2004; Ko and Kay, 2005; Lee and Kay, 2006) or EGF (Raymond et al., 1986), this approach has been deployed as a strategy to promote HCEC proliferation in order to engineer HCEC grafts for transplantation (Engelmann et al., 1988; Chen et al., 2001; Ishino et al., 2004; Mimura et al., 2004; Yokoo et al., 2005; Hsiue et al., 2006; Sumide et al., 2006; Li et al., 2007; Hatou et al., 2013). However, this conventional strategy frequently incites "pathological" EMT that turns HCECs into fibroblasts/myofibroblasts, leading to the formation of the retrocorneal membrane (Lee et al., 2004; Lee and Kay, 2006), and resorts to the use of either the ROCK inhibitor Y27632 (Okumura et al., 2012) or the TGF-βR blocker SB431542 (Okumura et al.,

2013) in order to avert EMT. This concern is consistent with our finding that EMT of HCECs is mediated by activation of canonical Wnt signaling during the proliferative phase but by activation of canonical TGF-β signaling during the irreversible nonproliferative phase (Zhu et al., 2012). Herein, we further raise this concern because even a brief EDTA/trypsin treatment still resulted in a "fibroblastic" appearance of HCECs that could not be reversed after extended culture in EGF-containing SHEM due to of rapid activation (within 24 to 48 h) of canonical Wnt signaling, which is indicated by increased TCF/LEF promoter activity, mRNA expression of β-catenin and LEF1, and nuclear translocation of β-catenin and LEF1 (Fig. 1). In contrast, HCEC monolayers treated by p120 siRNA or p120-Kaiso siRNAs retained a hexagonal shape without activation of canonical Wnt signaling (Fig. 1), a finding consistent with what we previously reported in HCECs (Zhu et al., 2012, 2014) and postconfluent ARPE-19 cells (Chen et al., 2012b).

p120 is the prototypic member of the subfamily of p120 armadillo-related proteins (Hatzfeld, 2005) associated with cadherin-mediated adherent junctions (Ireton et al., 2002; Davis et al., 2003; Xiao et al., 2003). Although the mechanism by which p120 affects Rho GTPases is still unclear, there is now strong evidence supporting the finding that p120 acts, at least in part, through regulation of Rho GTPases and its downstream target ROCK1/2 (Anastasiadis, 2007). Previous studies have shown a conflicting view, i.e., positive (Perez-Moreno et al., 2006, 2008; Wildenberg et al., 2006) or negative (Soto et al., 2008; Dohn et al., 2009) roles of p120 in cell proliferation. In HCECs, we noted that knockdown with p120 siRNA or p120-Kaiso siRNAs inhibited BrdU labeling if cell junctions were disrupted by EDTA/trypsin (Fig. S2), but promoted BrdU labeling by p120 siRNA (Zhu et al., 2012) or p120-Kaiso siRNAs (Zhu et al., 2014) in SHEM or MESCM (Fig. 2) when contact inhibition was maintained. Nuclear BrdU labeling is colocalized with nuclear translocation of p120, which also triggers nuclear release of Kaiso, suggesting the activation of p120-Kaiso signaling (Chen et al., 2012a; Zhu et al., 2012). Collectively, our studies suggest that the control of cell proliferation by p120 is largely contingent upon whether intercellular junctions of HCECs are perturbed or not.

In the event that contact inhibition is maintained, p120 plays a key role in controlling RhoA signaling passing from intercellular junctions to the nucleus, which may influence the control of contact inhibition (for reviews see Fagotto and Gumbiner, 1996; Jamora and Fuchs, 2002; Perez-Moreno et al., 2003; Matter et al., 2005). Consistent with this viewpoint, such activation of RhoA is required to elicit RhoA-ROCK signaling in order to unlock the mitotic block, as inhibition of RhoA by CT-04 or ROCK1/2 siRNAs abolished BrdU labeling and the ensuing expansion of HCEC monolayers cultured in SHEM (Fig. 2; Zhu et al., 2012, 2014). In SHEM, we have reported that the RhoA-ROCK signaling leads to activation of noncanonical BMP signaling that results in nuclear translocation of pNF-κB (Fig. 2) via the BMPRI–TAK1–XIAP complex (Hofer-Warbinek et al., 2000; Lu et al., 2007), as indicated by the cytoplasmic location of pSMAD1/5/8 as well as the lack of activation of ID1–4 (Zhu et al., 2014). In the present study, we conclude that unlocking the mitotic block via selective activation of the p120-Kaiso signaling in MESCM activates RhoA-ROCK-canonical BMP signaling. This is based on the finding that activation of RhoA-ROCK signaling is also necessary to unlock the mitotic block of HCEC monolayers when cultured in MESCM (Fig. 2). The RhoA-ROCK signaling did not lead to nuclear translocation of pNF-κB. Instead, it lead to nuclear translocation of pSMAD1/5/8 as a result of the activation of canonical BMP signaling, which is indicated by increased mRNA expression of BMP3, BMP4, and BMP6; enhanced mRNA and protein expression of BMPR1A and BMPR2; and up-regulation of the downstream SMAD-targeted genes ID1–4 (Fig. 2). Hence, the knockdown of p120 siRNA or p120-Kaiso siRNAs uniquely reveals a "physiological" signaling pathway that activates RhoA-ROCK signaling to unlock the mitotic block mediated in contact-inhibited HCEC monolayers. In EGF-containing SHEM, the RhoA-ROCK signaling triggers noncanonical BMP signaling and results in the expansion of HCEC monolayers to 5.0 ± 0.3 mm in diameter (Fig. 3 B). In bFGF/Leukemia inhibitory factor (LIF)-containing MESCM, however, the ensuing canonical BMP signaling resulted in marked expansion of HCEC monolayers to a transplantable size of 11.0 ± 0.6 mm in diameter (Fig. 3 B). Even at the end of 6 wk of culturing, the BrdU labeling index remained 40–50% in the midperipheral and peripheral zones, where contact inhibition might not be as fully established as the central zone (Fig. 3 C). The success of establishing such an effective expansion of HCEC monolayers that retained normal HCEC phenotype and an in vivo density upon withdrawal of p120-Kaiso siRNAs (Fig. 6) supports the feasibility of engineering eight additional HCEC grafts from one donor corneoscleral rim after corneal transplantation. We envision that the aforementioned discovery can be translated into a new technology of engineering HCEC surgical grafts to meet the global shortage of donor corneas.

Although there is a bona fide mitotic block of HCECs in vivo, tangential evidence has emerged suggesting the presence of HCEC progenitors in the corneal periphery or the junction between the corneal endothelium and the trabecular meshwork based on appearance of BrdU labeling (Whikehart et al., 2005), expression of stem cell markers such as Oct3/4 and Wnt1 (McGowan et al., 2007) after wounding, and formation of neurospheres with expression of nestin by EDTA-dissociated HCECs (Yokoo et al., 2005; Amano et al., 2006; Yamagami et al., 2007; Yu et al., 2011). For the first time, our study has disclosed the feasibility of promoting proliferation of HCEC monolayers by reprogramming adult HCECs into neural crest–like progenitors, as indicated by up-regulation of ESC markers such as Nanog, Nestin, Oct4, SOX-2, and SSEA4 as well as neural crest markers such as AP2β, FOXD3, and SOX9 in MESCM (Fig. 4), but not in SHEM (Fig. S3). Such reprogramming depended on the activation of canonical BMP signaling, as shown by the addition of Noggin (Fig. 4), which also aborted nuclear translocation of pSMAD1/5/8 and nuclear labeling of BrdU (Fig. 2), as well as by withdrawal of p120-Kaiso siRNAs for 1 wk (Fig. S1). Similar to what we have reported in SHEM (Zhu et al., 2012;Zhu et al., 2014), such withdrawal maintained an in vivo phenotype with a hexagonal shape and density (Fig. 6). The reprogrammed

HCECs can be induced to keratocyte-like cells expressing specific keratocyte markers such as keratocan, AQP1, B3GNT7, CHST7, and CD34 in a serum-free medium consisting of advanced MEM with 10 ng/ml bFGF and 0.1 mM ascorbic acid-2-phosphate (unpublished data), which supports the finding that they are neural crest–like progenitors.

Forced expression of transcription factors, e.g., Sox2, KLF4, Oct4, and c-Myc (SKOM), is a novel strategy (Takahashi et al., 2007) widely embraced by the scientific community to reprogram somatic cells to iPSCs for potential regenerative therapies (Drews et al., 2012; Iglesias-García et al., 2013). Induced pluripotency ensues through cooperation between expression of defined factors and the culture environment. Among all miRNAs, miR302 cluster, especially the member miR302b, acts on multiple targets to promote human somatic cell reprogramming (Subramanyam et al., 2011). In this process, Oct4, Sox2, and Nanog may directly bind to the promoter to activate expression of the miR302 cluster (Card et al., 2008; Barroso-delJesus et al., 2011), and the miR302 cluster indirectly induces expression of Oct4, Sox2, and Nanog by reducing the expression of developmental genes (Anokye-Danso et al., 2011; Lin et al., 2011). In HCEC monolayers, we noted that reprogramming by canonical BMP signaling was correlated with nuclear staining of Oct4, Sox2, and Nanog and up-regulation of miR302b more than miR302c (Fig. 4), which suggests that the positive autoregulatory feedback loop between miRNA302b and the Oct4–Sox2–Nanog complex might also operate in the reprogramming of HCEC progenitors. Future studies are needed to probe the linkage between RhoA-ROCK signaling and canonical BMP signaling in the activation of the reprogramming network of miRNA302b-Oct4-Sox2-Nanog. For example, ROCK1 and ROCK2, both downstream of RhoA and sharing 92% similarity in their kinase domains (Liao et al., 2007), might exert different effects from the miRNA 302b-Oct4-Sox2-Nanog network, as shown in regulation of BMPR1A, miR302c, Oct4, Sox2, and FOXD3 (Fig. 5). The signaling paradigm disclosed in our studies opens up a new way of thinking that some regenerative therapies may not need to reprogram somatic cells all the way to iPSCs.

Materials and methods

Materials

DMEM, Ham's/F12 medium, advance MEM, human EGF (hEGF), human bFGF (hbFGF), Noggin, Hepes buffer, HBSS, PBS, gentamicin, FBS, knockout serum, Texas red-X phalloidin, Alexa Fluor–conjugated secondary IgG, real-time PCR primers and probes, Kaiso (catalog no. 4392421, ID s19452), ROCK1 (catalog no. AM16708A, ID 14288) and ROCK2 siRNAs (catalog no. AM16708A, ID 110865), mirVana miRNA Isolation kit, NCode miRNA First-Strand cDNA Synthesis, qRT-PCR kits, and the monoclonal antibody against ZO-1 were purchased from Life Technologies. Collagenase A and insulin-transferrin-sodium selenite media supplement were obtained from Roche. Human LIF (hLIF), CT-04, ascorbic acid, laminin, hydrocortisone, dimethyl sulfoxide, cholera toxin, BSA, paraformaldehyde, methanol, Triton X-100, Hoechst 33342 dye, and monoclonal antibody against α-tubulin were obtained from Sigma-Aldrich. Collagen IV and monoclonal antibody against β-catenin were obtained from BD. Monoclonal antibodies against BrdU, Na-K-ATPase, and Oct4 were from Millipore. The monoclonal antibody against acetylated α-tubulin, BMPR1A, FOXD3, histone, Kaiso, nestin, SSEA4, and polyclonal antibodies against BMPR1B, BMPR2, γ-tubulin, LEF1, nanog, N-cadherin (type I), p75NTR, S100A4, Sox2, and Sox9 were obtained from Abcam. The polyclonal antibodies against α-catenin and p120 were purchased from Santa Cruz Biotechnology, Inc. The polyclonal antibody against RhoA and RhoA Activity Assay Biochem kit were obtained from Cytoskeleton, Inc. The polyclonal antibody against pNFkB (S276) and pSMAD1/5/8 was obtained from Cell Signaling Technology. The polyclonal antibody against keratocan was a gift from C. Liu (University of Cincinnati, Stetson, Cincinnati, OH). For details of the antibody sources, please see Table S1. An RNeasy Mini kit and HiPerFect siRNA transfection reagent were obtained from QIAGEN. A TCF/LEF reporter plasmid kit was purchased from SABiosciences. p120 siRNA was designed by us and obtained from Life Technologies with the target sequence of 5′-CAGAGGTGATCGCCATGCTTGGATT-3′.

HCEC isolation and culture

HCECs were isolated and cultured as described previously (Li et al., 2007; Zhu et al., 2008). In short, after corneal transplantation, the remaining corneoscleral rims were rinsed three times with DMEM containing 50 µg/ml gentamicin and 1.25 µg/ml amphotericin B. Under a dissecting microscope, the trabecular meshwork was cleaned up to the Schwalbe's line. The rim was cut into eight segments, from which the Descemet's membranes was stripped and digested at 37°C for 16 h with 1 mg/ml collagenase A in SHEM composed of an equal volume of DMEM and Ham's F12 supplemented with 5% FBS, 0.5% dimethyl sulfoxide, 2 ng/ml hEGF, 5 µg/ml insulin, 5 µg/ml transferrin, 5 ng/ml selenium, 0.5 mg/ml hydrocortisone, and 1 nM cholera toxin. The resultant aggregates of HCECs with undigested basement membrane matrix were collected by centrifugation at 2,000 rpm for 3 min to remove the digestion solution and cultured in 24-well dishes coated with collagen IV in SHEM or MESCM, which was made of DMEM/F-12 (1:1) supplemented with 10% knockout serum, 5 µg/ml insulin, 5 µg/ml transferrin, 5 ng/ml sodium selenite, 4 ng/ml bFGF, 10 ng/ml hLIF, 50 µg/ml gentamicin, and 1.25 µg/ml amphotericin B. Cultures were continuously monitored by phase-contrast microscopy. The size of the monolayers was determined by digitizing the surface area using ImageJ, and the cell counting was analyzed using Axio Vision software (Carl Zeiss).

siRNA transfection and other treatments

For the siRNA knockdown, parallel HCEC monolayers were subjected to weekly transfection by mixing 50 µl of serum-free, antibiotic-free SHEM or MESCM with 1 µl of HiPerFect siRNA transfection reagent (final dilution, 1:300) and 1.5 µl of 20 µM of scRNA, p120 siRNA, or p120-Kaiso siRNAs, each at the final concentration of 100 nM, drop-wise, followed by culturing in 250 µl of fresh SHEM or MESCM at 37°C. BrdU was added at a final concentration of 10 µM in the culture medium for 24 h before termination. Some cultures of HCECs were treated with p120-Kaiso siRNAs and 5 µg/ml CT-04, 100 nM of ROCK1 or ROCK2 siRNA, or 5 µg/ml Noggin simultaneously for 1 wk starting at 5 wk of culturing.

RNA extraction, reverse transcription, and real-time PCR

Total RNAs were extracted using an RNeasy Mini kit (QIAGEN) and reverse-transcribed using a High Capacity Reverse Transcription kit (Life Technologies). cDNA of each cell junction component was amplified by real-time RT-PCR using specific primer–probe mixtures and DNA polymerase in a real-time PCR system (7000; Life Technologies). The real-time RT-PCR profile consisted of 10 min of initial activation at 95°C, followed by 40 cycles of 15-s denaturation at 95°C, and 1 min annealing and extension at 60°C. The genuine identity of each PCR product was confirmed by the size determination using 2% agarose gels followed by ethidium bromide staining together with the PCR marker according to EC3 Imaging System (UVP, LLC).

TCF/LEF promoter assay

HCEC monolayers in 24-well dishes were cotransfected with 0.4% (wt/vol) of the TCF/LEF construct that harbors TCF/LEF-binding sites and 0.01% (wt/vol) of pRL-TK internal control plasmids with 1% (wt/vol) SuperFect plasmid transfection reagent in MESCM. After transfection for 24 h, cell lysates were assayed for firefly luciferase and Renilla luciferase activities using a Dual-Luciferase Reporter Assay System (Promega) and SpectralMax (Molecular Devices). The ratio of firefly luciferase and Renilla luciferase activities was used to determine whether the promoter was activated.

Immunostaining

HCEC monolayer cultures were air-dried and fixed in 4% formaldehyde, pH 7.0, for 15 min at room temperature, rehydrated in PBS, incubated with 0.2% Triton X-100 for 15 min, and rinsed three times with PBS for 5 min each. For double immunostaining of both BrdU and p120, samples were fixed with 75% methanol plus 25% acetic acid for 15 min, denatured with 2 M HCl for 30 min at 37°C, and neutralized by 0.1 M borate buffer, pH 8.5, for 5 min three times. After incubation with 2% BSA to block

nonspecific staining for 30 min, they were incubated with the desired first antibody (all at 1:50 dilution) for 16 h at 4°C. After three washes with PBS, they were incubated with corresponding Alexa Fluor–conjugated secondary IgG (all 1:100 dilution) for 60 min. The samples were then counterstained with Hoechst 33342 and analyzed with a confocal microscope (LSM 700; Carl Zeiss). Corresponding mouse and rabbit sera were used as negative controls for primary monoclonal and polyclonal antibodies, respectively.

Microscopy

An inverted microscope (Eclipse TS 100; Nikon) was used for phase contrast images. The objective lenses used were from Modulation Optics Inc., and were HMC 10× Plan/0.25 NA. The images were taken at room temperature. The image medium was a culture medium such as MESCM. No fluorochromes were used for phase contrast images. The camera used was a Retiga 2000 R (QImaging). The acquisition software was QCapture Pro 6.0 (QImaging). The software for imaging process subsequent to data acquisition was Photoshop CS6 (Adobe).

A confocal microscope (LSM; Carl Zeiss) was used for confocal images. The objective lenses used were LD plan-Neo fluor, 20×/0.4 NA Korr, or EC Plan-neo fluor 40× 1.3 NA oil differential interference contrast (DIC) for higher power images. The images were taken at room temperature. The image medium was Vectashield H-1000. For higher power images (40×), Immorsal 518 N (Carl Zeiss) was also used. The fluorochromes used were Streptavidin Alexa 488 and Streptavidin Alexa 555 conjugated to the secondary antibodies for confocal images (Invitrogen). The camera used was an LSM T-PMT (Carl Zeiss). The acquisition software was Zen Black-Confocal (Carl Zeiss). The software for imaging process subsequent to data acquisition was Photoshop CS6.

RhoA activity assay

The assay of Rho activation was performed in 10–50 µg of cell lysate protein using a RhoA Activation Assay Biochem kit to pull down the GTP-bound form of RhoA with a GST fusion protein containing rhotekin (7–89 residues) and ras binding domain (RBD) protein using brightly colored glutathione affinity beads. The amount of activated RhoA pulled down was quantitatively determined by Western blotting using anti-RhoA antibody.

Expression of miR302

miRNAs were isolated using a mirVana miRNA Isolation kit (Life Technologies). Both miR-302b and miR-302c were quantified by qRT-PCR using NCode miRNA First-Strand cDNA Synthesis and qRT-PCR kits (Life Technologies).

Western blotting

Cell lysates were prepared in RIPA buffer and resolved on 4–15% (wt/vol) gradient acrylamide gels under denaturing and reducing conditions for Western blotting. The protein extracts were transferred to a nitrocellulose membrane, which was then blocked with 5% (wt/vol) fat-free milk in TBST (50 mM Tris-HCl, pH 7.5, 150 mM NaCl, and 0.05% [vol/vol] Tween-20), followed by sequential incubation with specific primary antibodies against BMPR1A, BMPR1B, BMPR2, and RhoA and their respective secondary antibodies using α-tubulin or histone as the loading control. Immunoreactive proteins were detected with Western Lighting Chemiluminescence (PerkinElmer).

Statistical analysis

All summary data were reported as means ± SD calculated for each group and compared using ANOVA and the Student's paired and unpaired *t* test using Excel software (Microsoft). Test results were reported as two-tailed p-values, where $P < 0.05$ was considered statistically significant.

Online supplemental materials

Fig. S1 shows cessation of Rho-BMP signaling and expression of neural crest and ESC markers 1 wk after withdrawal of p120 or p120-Kaiso siRNA. Fig. S2 shows inhibition of BrdU labeling in trypsin-EDTA–treated HCECs treated with p120 or p120-Kaiso siRNA. Fig. S3 shows lack of reprogramming in HCECs treated with p120 or p120-Kaiso siRNA when cultured in SHEM. Online supplemental material is available at http://www.jcb.org/cgi/content/full/jcb.201404032/DC1.

The work in this article was supported by R43 EY022502-01 and R44 EY022502-02 grants from the National Eye Institute, National Institutes of Health (Y.T. Zhu and S.C.G. Tseng), and a research grant from TissueTech, Inc. S.C.G. Tseng, Y. Zhu, and W. Li have filed a PCT patent application on Sept. 27, 2007, titled "RNAi Methods and Compositions for Stimulating Proliferation of Cells with Adherent Functions."

The authors declare no further competing financial interests.

Submitted: 7 April 2014
Accepted: 5 August 2014

References

Amano, S., S. Yamagami, T. Mimura, S. Uchida, and S. Yokoo. 2006. Corneal stromal and endothelial cell precursors. *Cornea*. 25(10, Suppl 1):S73–S77. http://dx.doi.org/10.1097/01.ico.0000247218.10672.7e

Anastasiadis, P.Z. 2007. p120-ctn: A nexus for contextual signaling via Rho GTPases. *Biochim. Biophys. Acta*. 1773:34–46. http://dx.doi.org/10.1016/j.bbamcr.2006.08.040

Anokye-Danso, F., C.M. Trivedi, D. Juhr, M. Gupta, Z. Cui, Y. Tian, Y. Zhang, W. Yang, P.J. Gruber, J.A. Epstein, and E.E. Morrisey. 2011. Highly efficient miRNA-mediated reprogramming of mouse and human somatic cells to pluripotency. *Cell Stem Cell*. 8:376–388. http://dx.doi.org/10.1016/j.stem.2011.03.001

Barroso-delJesus, A., G. Lucena-Aguilar, L. Sanchez, G. Ligero, I. Gutierrez-Aranda, and P. Menendez. 2011. The Nodal inhibitor Lefty is negatively modulated by the microRNA miR-302 in human embryonic stem cells. *FASEB J.* 25:1497–1508. http://dx.doi.org/10.1096/fj.10-172221

Blitzer, A.L., L. Panagis, G.L. Gusella, J. Danias, M. Mlodzik, and C. Iomini. 2011. Primary cilia dynamics instruct tissue patterning and repair of corneal endothelium. *Proc. Natl. Acad. Sci. USA*. 108:2819–2824. http://dx.doi.org/10.1073/pnas.1016702108

Bonanno, J.A. 2003. Identity and regulation of ion transport mechanisms in the corneal endothelium. *Prog. Retin. Eye Res.* 22:69–94. http://dx.doi.org/10.1016/S1350-9462(02)00059-9

Bourne, W.M., and J.W. McLaren. 2004. Clinical responses of the corneal endothelium. *Exp. Eye Res.* 78:561–572. http://dx.doi.org/10.1016/j.exer.2003.08.002

Card, D.A., P.B. Hebbar, L. Li, K.W. Trotter, Y. Komatsu, Y. Mishina, and T.K. Archer. 2008. Oct4/Sox2-regulated miR-302 targets cyclin D1 in human embryonic stem cells. *Mol. Cell. Biol.* 28:6426–6438. http://dx.doi.org/10.1128/MCB.00359-08

Chen, K.H., D. Azar, and N.C. Joyce. 2001. Transplantation of adult human corneal endothelium ex vivo: a morphologic study. *Cornea*. 20:731–737. http://dx.doi.org/10.1097/00003226-200110000-00012

Chen, H.C., Y.T. Zhu, S.Y. Chen, and S.C. Tseng. 2012a. Selective activation of p120ctn-Kaiso signaling to unlock contact inhibition of ARPE-19 cells without epithelial-mesenchymal transition. *PLoS ONE*. 7:e36864. http://dx.doi.org/10.1371/journal.pone.0036864

Chen, H.C., Y.T. Zhu, S.Y. Chen, and S.C. Tseng. 2012b. Wnt signaling induces epithelial-mesenchymal transition with proliferation in ARPE-19 cells upon loss of contact inhibition. *Lab. Invest.* 92:676–687. http://dx.doi.org/10.1038/labinvest.2011.201

Daniel, J.M. 2007. Dancing in and out of the nucleus: p120(ctn) and the transcription factor Kaiso. *Biochim. Biophys. Acta*. 1773:59–68. http://dx.doi.org/10.1016/j.bbamcr.2006.08.052

Davis, M.A., R.C. Ireton, and A.B. Reynolds. 2003. A core function for p120-catenin in cadherin turnover. *J. Cell Biol.* 163:525–534. http://dx.doi.org/10.1083/jcb.200307111

Dohn, M.R., M.V. Brown, and A.B. Reynolds. 2009. An essential role for p120-catenin in Src- and Rac1-mediated anchorage-independent cell growth. *J. Cell Biol.* 184:437–450. http://dx.doi.org/10.1083/jcb.200807096

Drews, K., J. Jozefczuk, A. Prigione, and J. Adjaye. 2012. Human induced pluripotent stem cells—from mechanisms to clinical applications. *J. Mol. Med.* 90:735–745. http://dx.doi.org/10.1007/s00109-012-0913-0

Engelmann, K., M. Böhnke, and P. Friedl. 1988. Isolation and long-term cultivation of human corneal endothelial cells. *Invest. Ophthalmol. Vis. Sci.* 29:1656–1662.

Fagotto, F., and B.M. Gumbiner. 1996. Cell contact-dependent signaling. *Dev. Biol.* 180:445–454. http://dx.doi.org/10.1006/dbio.1996.0318

Fischbarg, J., and D.M. Maurice. 2004. An update on corneal hydration control. *Exp. Eye Res.* 78:537–541. http://dx.doi.org/10.1016/j.exer.2003.09.010

Hatou, S., S. Yoshida, K. Higa, H. Miyashita, E. Inagaki, H. Okano, K. Tsubota, and S. Shimmura. 2013. Functional corneal endothelium derived from corneal stroma stem cells of neural crest origin by retinoic acid and Wnt/β-catenin signaling. *Stem Cells Dev.* 22:828–839. http://dx.doi.org/10.1089/scd.2012.0286

Hatzfeld, M. 2005. The p120 family of cell adhesion molecules. *Eur. J. Cell Biol.* 84:205–214. http://dx.doi.org/10.1016/j.ejcb.2004.12.016

Hofer-Warbinek, R., J.A. Schmid, C. Stehlik, B.R. Binder, J. Lipp, and R. de Martin. 2000. Activation of NF-kappa B by XIAP, the X chromosome-linked inhibitor of apoptosis, in endothelial cells involves TAK1. *J. Biol. Chem.* 275:22064–22068. http://dx.doi.org/10.1074/jbc.M910346199

Hollnagel, A., V. Oehlmann, J. Heymer, U. Rüther, and A. Nordheim. 1999. Id genes are direct targets of bone morphogenetic protein induction in embryonic stem cells. *J. Biol. Chem.* 274:19838–19845. http://dx.doi.org/10.1074/jbc.274.28.19838

Hsiue, G.H., J.Y. Lai, K.H. Chen, and W.M. Hsu. 2006. A novel strategy for corneal endothelial reconstruction with a bioengineered cell sheet. *Transplantation*. 81:473–476. http://dx.doi.org/10.1097/01.tp.0000194864.13539.2c

Iglesias-García, O., B. Pelacho, and F. Prósper. 2013. Induced pluripotent stem cells as a new strategy for cardiac regeneration and disease modeling. *J. Mol. Cell. Cardiol.* 62:43–50. http://dx.doi.org/10.1016/j.yjmcc.2013.04.022

Ireton, R.C., M.A. Davis, J. van Hengel, D.J. Mariner, K. Barnes, M.A. Thoreson, P.Z. Anastasiadis, L. Matrisian, L.M. Bundy, L. Sealy, et al. 2002. A novel role for p120 catenin in E-cadherin function. *J. Cell Biol.* 159:465–476. http://dx.doi.org/10.1083/jcb.200205115

Ishino, Y., Y. Sano, T. Nakamura, C.J. Connon, H. Rigby, N.J. Fullwood, and S. Kinoshita. 2004. Amniotic membrane as a carrier for cultivated human corneal endothelial cell transplantation. *Invest. Ophthalmol. Vis. Sci.* 45:800–806. http://dx.doi.org/10.1167/iovs.03-0016

Jamora, C., and E. Fuchs. 2002. Intercellular adhesion, signalling and the cytoskeleton. *Nat. Cell Biol.* 4:E101–E108.

Joyce, N.C. 2005. Cell cycle status in human corneal endothelium. *Exp. Eye Res.* 81:629–638. http://dx.doi.org/10.1016/j.exer.2005.06.012

Kay, E.P., M.S. Lee, G.J. Seong, and Y.G. Lee. 1998. TGF-βs stimulate cell proliferation via an autocrine production of FGF-2 in corneal stromal fibroblasts. *Curr. Eye Res.* 17:286–293. http://dx.doi.org/10.1076/ceyr.17.3.286.5212

Ko, M.K., and E.P. Kay. 2005. Regulatory role of FGF-2 on type I collagen expression during endothelial mesenchymal transformation. *Invest. Ophthalmol. Vis. Sci.* 46:4495–4503. http://dx.doi.org/10.1167/iovs.05-0818

Laing, R.A., L. Neubauer, S.S. Oak, H.L. Kayne, and H.M. Leibowitz. 1984. Evidence for mitosis in the adult corneal endothelium. *Ophthalmology*. 91:1129–1134. http://dx.doi.org/10.1016/S0161-6420(84)34176-8

Lee, J.G., and E.P. Kay. 2006. FGF-2-mediated signal transduction during endothelial mesenchymal transformation in corneal endothelial cells. *Exp. Eye Res.* 83:1309–1316. http://dx.doi.org/10.1016/j.exer.2006.04.007

Lee, H.T., J.G. Lee, M. Na, and E.P. Kay. 2004. FGF-2 induced by interleukin-1β through the action of phosphatidylinositol 3-kinase mediates endothelial mesenchymal transformation in corneal endothelial cells. *J. Biol. Chem.* 279:32325–32332. http://dx.doi.org/10.1074/jbc.M405208200

Li, W., A.L. Sabater, Y.T. Chen, Y. Hayashida, S.Y. Chen, H. He, and S.C. Tseng. 2007. A novel method of isolation, preservation, and expansion of human corneal endothelial cells. *Invest. Ophthalmol. Vis. Sci.* 48:614–620. http://dx.doi.org/10.1167/iovs.06-1126

Li, G.G., S.Y. Chen, H.T. Xie, Y.T. Zhu, and S.C. Tseng. 2012a. Angiogenesis potential of human limbal stromal niche cells. *Invest. Ophthalmol. Vis. Sci.* 53:3357–3367. http://dx.doi.org/10.1167/iovs.11-9414

Li, G.G., Y.T. Zhu, H.T. Xie, S.Y. Chen, and S.C. Tseng. 2012b. Mesenchymal stem cells derived from human limbal niche cells. *Invest. Ophthalmol. Vis. Sci.* 53:5686–5697. http://dx.doi.org/10.1167/iovs.12-10300

Liao, J.K., M. Seto, and K. Noma. 2007. Rho kinase (ROCK) inhibitors. *J. Cardiovasc. Pharmacol.* 50:17–24. http://dx.doi.org/10.1097/FJC.0b013e318070d1bd

Lin, S.L., D.C. Chang, C.H. Lin, S.Y. Ying, D. Leu, and D.T. Wu. 2011. Regulation of somatic cell reprogramming through inducible mir-302 expression. *Nucleic Acids Res.* 39:1054–1065. http://dx.doi.org/10.1093/nar/gkq850

Lu, M., S.C. Lin, Y. Huang, Y.J. Kang, R. Rich, Y.C. Lo, D. Myszka, J. Han, and H. Wu. 2007. XIAP induces NF-κB activation via the BIR1/TAB1 interaction and BIR1 dimerization. *Mol. Cell*. 26:689–702. http://dx.doi.org/10.1016/j.molcel.2007.05.006

Matter, K., S. Aijaz, A. Tsapara, and M.S. Balda. 2005. Mammalian tight junctions in the regulation of epithelial differentiation and proliferation. *Curr. Opin. Cell Biol.* 17:453–458. http://dx.doi.org/10.1016/j.ceb.2005.08.003

McGowan, S.L., H.F. Edelhauser, R.R. Pfister, and D.R. Whikehart. 2007. Stem cell markers in the human posterior limbus and corneal endothelium of unwounded and wounded corneas. *Mol. Vis.* 13:1984–2000.

Mimura, T., S. Yamagami, S. Yokoo, T. Usui, K. Tanaka, S. Hattori, S. Irie, K. Miyata, M. Araie, and S. Amano. 2004. Cultured human corneal endothelial cell transplantation with a collagen sheet in a rabbit model. *Invest. Ophthalmol. Vis. Sci.* 45:2992–2997. http://dx.doi.org/10.1167/iovs.03-1174

Miyoshi, N., H. Ishii, H. Nagano, N. Haraguchi, D.L. Dewi, Y. Kano, S. Nishikawa, M. Tanemura, K. Mimori, F. Tanaka, et al. 2011. Reprogramming of mouse and human cells to pluripotency using mature microRNAs. *Cell Stem Cell*. 8:633–638. http://dx.doi.org/10.1016/j.stem.2011.05.001

Okumura, N., N. Koizumi, M. Ueno, Y. Sakamoto, H. Takahashi, H. Tsuchiya, J. Hamuro, and S. Kinoshita. 2012. ROCK inhibitor converts corneal endothelial cells into a phenotype capable of regenerating in vivo endothelial tissue. *Am. J. Pathol.* 181:268–277. http://dx.doi.org/10.1016/j.ajpath.2012.03.033

Okumura, N., E.P. Kay, M. Nakahara, J. Hamuro, S. Kinoshita, and N. Koizumi. 2013. Inhibition of TGF-β signaling enables human corneal endothelial cell expansion in vitro for use in regenerative medicine. *PLoS ONE*. 8:e58000. http://dx.doi.org/10.1371/journal.pone.0058000

Patel, S.P., and W.M. Bourne. 2009. Corneal endothelial cell proliferation: a function of cell density. *Invest. Ophthalmol. Vis. Sci.* 50:2742–2746. http://dx.doi.org/10.1167/iovs.08-3002

Perez-Moreno, M., C. Jamora, and E. Fuchs. 2003. Sticky business: orchestrating cellular signals at adherens junctions. *Cell*. 112:535–548. http://dx.doi.org/10.1016/S0092-8674(03)00108-9

Perez-Moreno, M., M.A. Davis, E. Wong, H.A. Pasolli, A.B. Reynolds, and E. Fuchs. 2006. p120-catenin mediates inflammatory responses in the skin. *Cell*. 124:631–644. http://dx.doi.org/10.1016/j.cell.2005.11.043

Perez-Moreno, M., W. Song, H.A. Pasolli, S.E. Williams, and E. Fuchs. 2008. Loss of p120 catenin and links to mitotic alterations, inflammation, and skin cancer. *Proc. Natl. Acad. Sci. USA*. 105:15399–15404. http://dx.doi.org/10.1073/pnas.0807301105

Raymond, G.M., M.M. Jumblatt, S.P. Bartels, and A.H. Neufeld. 1986. Rabbit corneal endothelial cells in vitro: effects of EGF. *Invest. Ophthalmol. Vis. Sci.* 27:474–479.

Senoo, T., Y. Obara, and N.C. Joyce. 2000. EDTA: a promoter of proliferation in human corneal endothelium. *Invest. Ophthalmol. Vis. Sci.* 41: 2930–2935.

Soto, E., M. Yanagisawa, L.A. Marlow, J.A. Copland, E.A. Perez, and P.Z. Anastasiadis. 2008. p120 catenin induces opposing effects on tumor cell growth depending on E-cadherin expression. *J. Cell Biol.* 183:737–749. http://dx.doi.org/10.1083/jcb.200805113

Stiles, J.M., V. Kurisetty, D.C. Mitchell, and B.A. Bryan. 2013. Rho kinase proteins regulate global miRNA expression in endothelial cells. *Cancer Genomics Proteomics*. 10:251–263.

Subramanyam, D., S. Lamouille, R.L. Judson, J.Y. Liu, N. Bucay, R. Derynck, and R. Blelloch. 2011. Multiple targets of miR-302 and miR-372 promote reprogramming of human fibroblasts to induced pluripotent stem cells. *Nat. Biotechnol.* 29:443–448. http://dx.doi.org/10.1038/nbt.1862

Sumide, T., K. Nishida, M. Yamato, T. Ide, Y. Hayashida, K. Watanabe, J. Yang, C. Kohno, A. Kikuchi, N. Maeda, et al. 2006. Functional human corneal endothelial cell sheets harvested from temperature-responsive culture surfaces. *FASEB J.* 20:392–394.

Takahashi, K., K. Tanabe, M. Ohnuki, M. Narita, T. Ichisaka, K. Tomoda, and S. Yamanaka. 2007. Induction of pluripotent stem cells from adult human fibroblasts by defined factors. *Cell*. 131:861–872. http://dx.doi.org/10.1016/j.cell.2007.11.019

Whikehart, D.R., C.H. Parikh, A.V. Vaughn, K. Mishler, and H.F. Edelhauser. 2005. Evidence suggesting the existence of stem cells for the human corneal endothelium. *Mol. Vis.* 11:816–824.

Wildenberg, G.A., M.R. Dohn, R.H. Carnahan, M.A. Davis, N.A. Lobdell, J. Settleman, and A.B. Reynolds. 2006. p120-catenin and p190RhoGAP regulate cell-cell adhesion by coordinating antagonism between Rac and Rho. *Cell*. 127:1027–1039. http://dx.doi.org/10.1016/j.cell.2006.09.046

Wong, C.E., C. Paratore, M.T. Dours-Zimmermann, A. Rochat, T. Pietri, U. Suter, D.R. Zimmermann, S. Dufour, J.P. Thiery, D. Meijer, et al. 2006. Neural crest-derived cells with stem cell features can be traced back to multiple lineages in the adult skin. *J. Cell Biol.* 175:1005–1015. http://dx.doi.org/10.1083/jcb.200606062

Xiao, K., D.F. Allison, K.M. Buckley, M.D. Kottke, P.A. Vincent, V. Faundez, and A.P. Kowalczyk. 2003. Cellular levels of p120 catenin function as a set point for cadherin expression levels in microvascular endothelial cells. *J. Cell Biol.* 163:535–545. http://dx.doi.org/10.1083/jcb.200306001

Xie, H.T., S.Y. Chen, G.G. Li, and S.C. Tseng. 2011. Limbal epithelial stem/progenitor cells attract stromal niche cells by SDF-1/CXCR4 signaling to prevent differentiation. *Stem Cells*. 29:1874–1885. http://dx.doi.org/10.1002/stem.743

Xie, H.T., S.Y. Chen, G.G. Li, and S.C. Tseng. 2012. Isolation and expansion of human limbal stromal niche cells. *Invest. Ophthalmol. Vis. Sci.* 53:279–286. http://dx.doi.org/10.1167/iovs.11-8441

Yamagami, S., S. Yokoo, T. Mimura, T. Takato, M. Araie, and S. Amano. 2007. Distribution of precursors in human corneal stromal cells and endothelial cells. *Ophthalmology*. 114:433–439. http://dx.doi.org/10.1016/j.ophtha.2006.07.042

Yokoo, S., S. Yamagami, Y. Yanagi, S. Uchida, T. Mimura, T. Usui, and S. Amano. 2005. Human corneal endothelial cell precursors isolated by sphere-forming assay. *Invest. Ophthalmol. Vis. Sci.* 46:1626–1631. http://dx.doi.org/10.1167/iovs.04-1263

Yu, W.Y., C. Sheridan, I. Grierson, S. Mason, V. Kearns, A.C. Lo, and D. Wong. 2011. Progenitors for the corneal endothelium and trabecular meshwork: a potential source for personalized stem cell therapy in corneal endothelial diseases and glaucoma. *J. Biomed. Biotechnol.* 2011:412743. http://dx.doi.org/10.1155/2011/412743

Zhu, Y.T., Y. Hayashida, A. Kheirkhah, H. He, S.Y. Chen, and S.C. Tseng. 2008. Characterization and comparison of intercellular adherent junctions expressed by human corneal endothelial cells in vivo and in vitro. *Invest. Ophthalmol. Vis. Sci.* 49:3879–3886. http://dx.doi.org/10.1167/iovs.08-1693

Zhu, Y.T., H.C. Chen, S.Y. Chen, and S.C. Tseng. 2012. Nuclear p120 catenin unlocks mitotic block of contact-inhibited human corneal endothelial monolayers without disrupting adherent junctions. *J. Cell Sci.* 125:3636–3648. http://dx.doi.org/10.1242/jcs.103267

Zhu, Y.T., B. Han, F. Li, S.Y. Chen, S. Tighe, S. Zhang, and S.C. Tseng. 2014. Knockdown of both p120 catenin and Kaiso promotes expansion of human corneal endothelial monolayers via RhoA-ROCK-noncanonical BMP-NFκB pathway. *Invest. Ophthalmol. Vis. Sci.* 55:1509–1518. http://dx.doi.org/10.1167/iovs.13-13633

Zhu et al., http://www.jcb.org/cgi/content/full/jcb.201404032/DC1

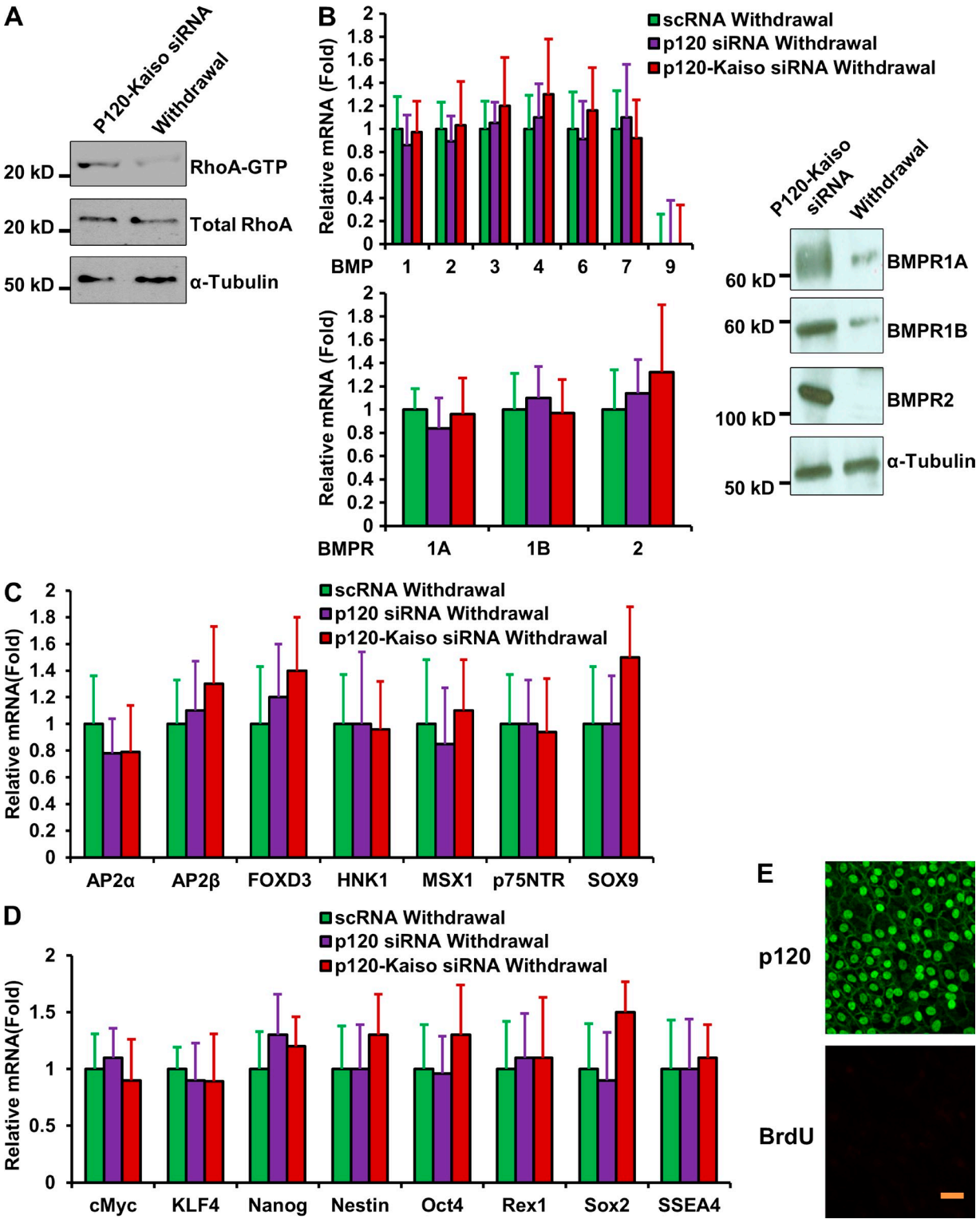

Figure S1. **Cessation of Rho-BMP signaling and expression of neural crest and ESC markers after withdrawal.** The resultant HCEC monolayers after withdrawal were investigated for the level of RhoA-GTP by Western blotting (A; using α-tubulin as the loading control); for the transcript and protein expression of BMP ligands and receptors by qRT-PCR and Western blot, respectively (B; $P > 0.05$, $n = 4$, using α-tubulin as the loading control); for the transcript expression of ESC markers (C) and neural crest markers (D) by qRT-PCR; and for double immunostaining to p120 (green) and BrdU (red; E). Error bars indicate ±SEM. Bars, 25 µm.

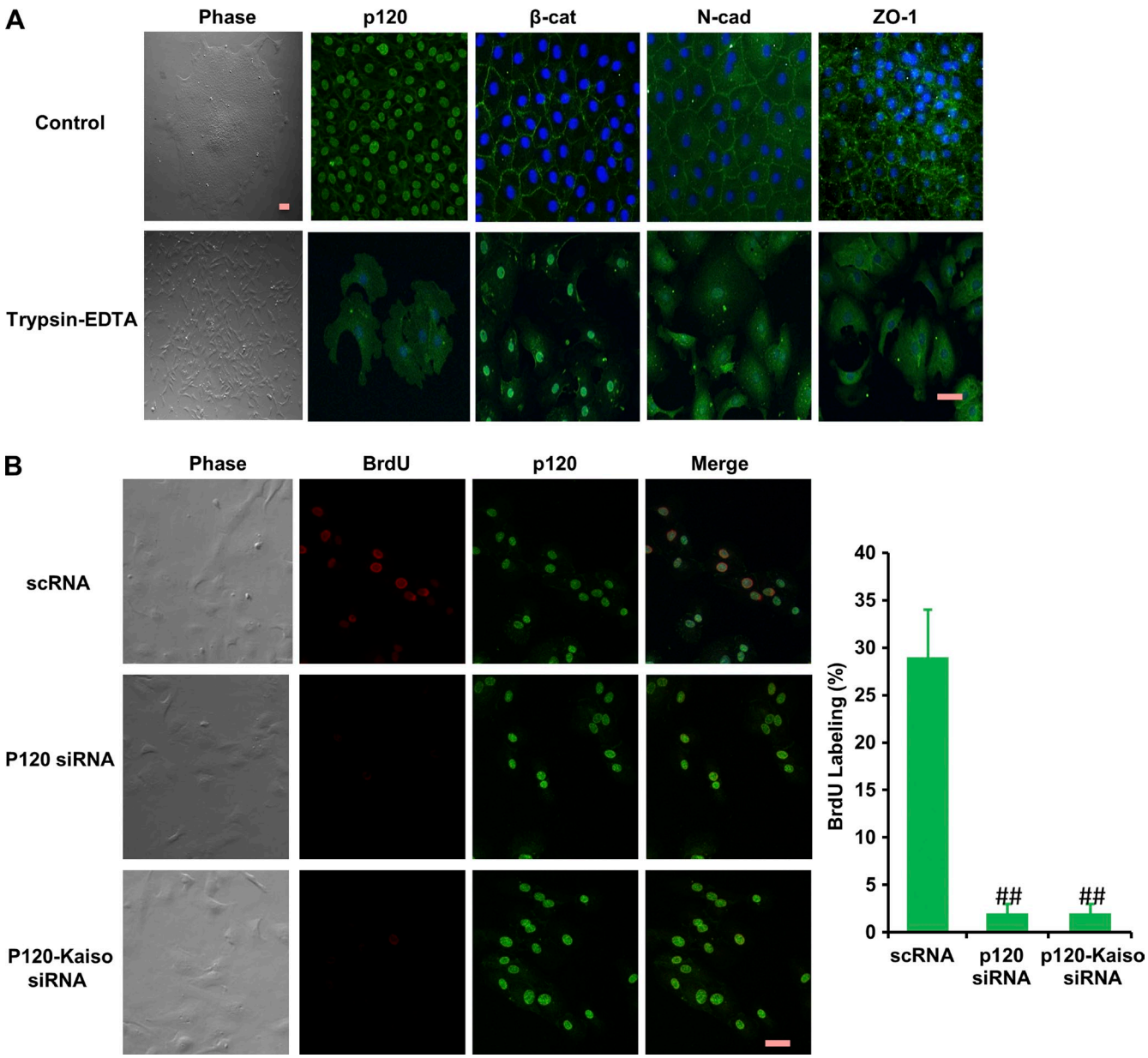

Figure S2. **BrdU labeling in trypsin-EDTA–treated HCECs inhibited by p120-Kaiso siRNAs.** Trypsin-EDTA disrupted the hexagonal shape and altered the intercellular expression pattern of p120, β-catenin, N-cadherin, and ZO-1 in the HCEC monolayer cultured in SHEM for 1 d (A). The BrdU-labeled nuclei noted in fibroblastic-like cells were significantly reduced by knockdown with p120 siRNA and p120-Kaiso siRNAs, but not scRNA, for 2 d (B; ##, $P < 0.01$; $n = 4$). Error bars indicate ±SEM. Bars, 25 µm.

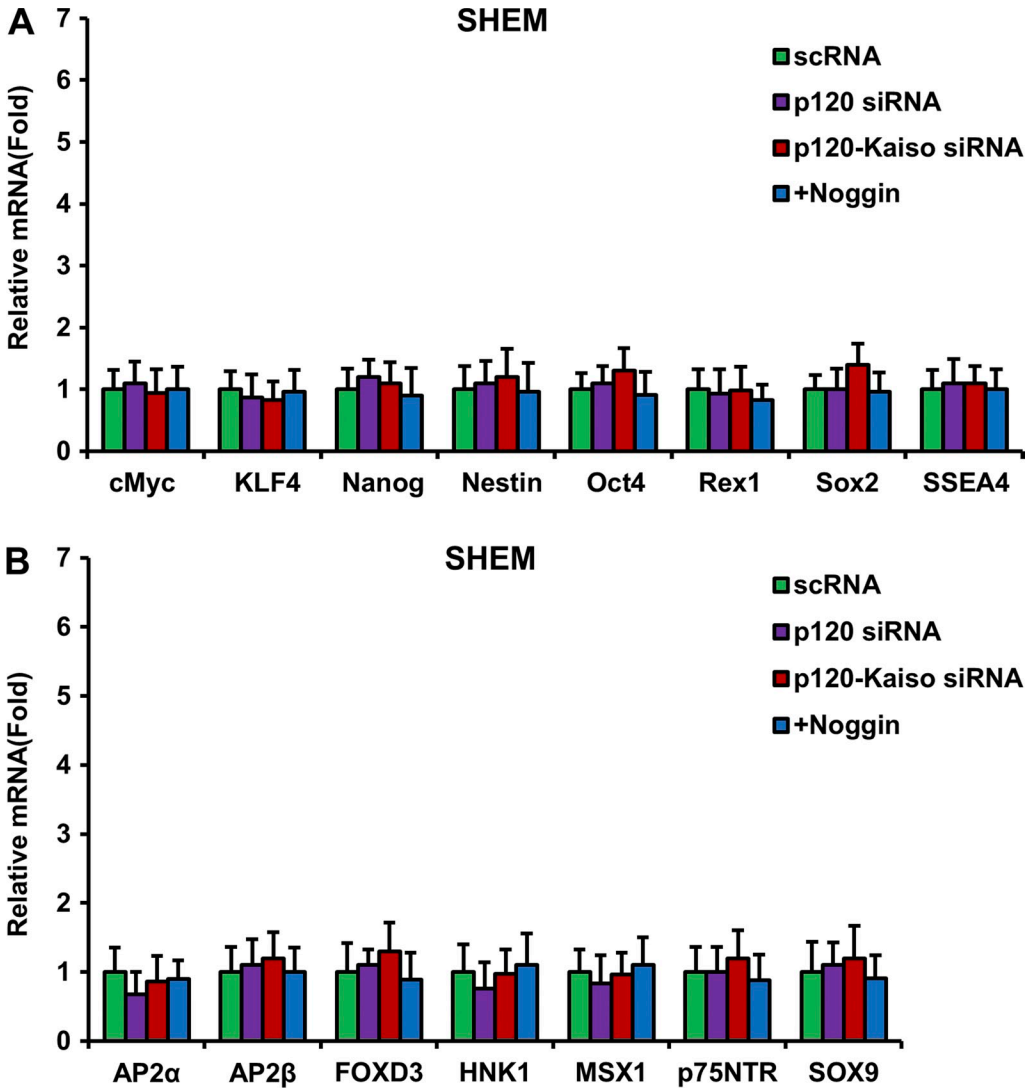

Figure S3. **Lack of reprogramming by p120 or p120-Kaiso siRNA knockdown in SHEM.** HCEC monolayers received weekly knockdown by p120 siRNA or p120-Kaiso siRNAs starting at 1 wk of culturing in SHEM. Transcript expression of ESC markers (A) and neural crest cell markers (B) was measured by qRT-PCR after 5 wk of culturing when 5 μg/ml Noggin was added for the last week. Error bars indicate ±SEM.

Table S1. **Commercial sources of antibodies**

Antibody	Vendor	Source	Catalog number
α-Catenin	Santa Cruz Biotechnology, Inc.	Goat	SC-1498
α-Tubulin	Sigma-Aldrich	Mouse	T9026
Acetylated α-tubulin	Abcam	Mouse	ab24610
β-Catenin	BD	Mouse	610154
BMPR1A	Abcam	Mouse	ab166707
BMPR1B	Abcam	Rabbit	ab1555058
BMPR2	Abcam	Rabbit	ab106266
BrdU	EMD Millipore	Mouse	MAB3222
FOXD3	Abcam	Mouse	ab107248
Γ-Catenin	Abcam	Goat	ab11799
Histone	Abcam	Mouse	ab10799
Kaiso	Abcam	Mouse	ab12723
LEF1	Abcam	Rabbit	ab53293
Na-K-ATPase	EMD Millipore	Mouse	05-369
Nanog	Abcam	Rabbit	ab80892
N-cadherin	Santa Cruz Biotechnology, Inc.	Rabbit	SC-7939
Nestin	Abcam	Mouse	ab22035
Oct4	EMD Millipore	Mouse	MAB4419
p120	Santa Cruz Biotechnology, Inc.	Rabbit	SC1101
p75NTR	Abcam	Rabbit	ab8874
pNFkB (S276)	Cell Signaling Technology	Rabbit	3037S
pSMAD1/5/8	Cell Signaling Technology	Rabbit	9511S